Thermal and mechanical properties of hybrid methylsilsesquioxane/poly(styrene-b-4-vinylpyridine) low-*k* dielectrics using a late porogen removal scheme

Mu-Lung Che, Cheng-Ying Huang, Shindy Choang, Yu-Hen Chen, and Jihperng Leu[a)]
Department of Materials Science and Engineering, National Chiao Tung University, Hsinchu, Taiwan 30010

(Received 14 November 2009; accepted 3 February 2010)

A late porogen removal scheme was used to make low-*k* materials ($k = 2.72$ to 2.02) using methylsilsesquioxane (MSQ) and a high-temperature porogen, poly(styrene-b-4-vinylpyridine) (PS-b-P4VP), to circumvent the reliability issues related to as-deposited porous dielectric. Based on the nanoindentation and Fourier transform infrared spectroscopy (FTIR) analysis, the moduli of the hybrid films were found to be higher than their porous forms, and even better than the dense MSQ film, for porogen loading below a critical level (~69.5 vol%). This could be attributed to their enhanced degree of cross-linking in MSQ as evidenced by the network/cage structural ratios. Besides, high-temperature porogen plays different roles during the cross-linking of MSQ depending on its loadings. In this study, with immediate loading at 16.7 vol%, PS-b-P4VP can serve as plasticizer to enhance the degree of cross-linking, but at a large loading >16.7 vol%, it becomes a steric hindrance reducing the degree of cross-linking.

I. INTRODUCTION

As the feature size in microelectronic devices is scaled down, the increase of propagation (RC) delay in the backend interconnect becomes the limiting factor of delay.[1] To minimize the increase of RC delay, the industry first introduced copper metallization to reduce the resistance as well as improve the electromigration performance of wiring.[2] To continually reduce the RC delay of interconnects, low dielectric constant (low-*k*) materials such as carbon-doped oxide (CDO)[3] or SiLK,[4] a polyphenylene polymer, with *k* ranging from 2.65 to 3.2, have been introduced primarily in 90 nm node to replace the interlayer dielectric (ILD), SiO_2 ($k \approx 4.0$) or fluorosilicate glass ($k \approx 3.7$).[5] Further reduction of the effective *k* in dual damascene interconnection involves the scaling of *k* value and the film thickness of the etch-stop layer[6] in addition to the traditional scaling of ILD materials in a 65 nm node. For 45 nm technology node and beyond, it is well recognized that the incorporation of porosity ($k_{air} = 1$) is critical to the search for viable low-*k* dielectrics ultralow-*k* materials with $k < 2.4$, according to the 2007 International Technology Roadmap for Semiconductors (ITRS).[7]

One practical approach for creating porous structure in spin-on low-*k* dielectrics is through a pore generator (porogen), which is removed at low temperatures, typically ≤200 °C immediately after the film deposition, using porogens such as norbornene-derivative,[8] polyoxyethylene ether,[9] and amphiphilic block copolymers (ABC) such as poly(methyl methacrylate-co-dimethylaminoethyl methacrylate) (PMMA-co-PDMAEMA) and poly(ethylene oxide-b-propylene oxide-b-ethylene oxide) (PEO-b-PPO-b-PEO).[10,11] Specifically, it has been demonstrated that the amphiphilic characteristic of ABCs with low decomposition temperature can significantly improve the miscibility with low-*k* matrices such as methylsilsesquioxane (MSQ) such that significant aggregation cannot occur before curing.[12,13]

Although the ABCs such as PEO-b-PPO-b-PEO have been successfully used as porogens for fabrication of porous low-*k* film, several serious issues related to as-deposited porous dielectrics ($k < 2.5$) have been identified in the process of their integration; namely: (i) device reliability at barrier/low-*k* interface resulting from large pore size (>15 Å), and (ii) RC variation resulting from roughness in the dielectric from etching.[14] To circumvent these problems, a novel postintegration porogen removal approach in materials and integration; i.e., a late porogen removal scheme has been proposed using a high-temperature porogen to defer the formation of porous low-*k* dielectric after the CMP step, and then thermally remove the sacrificial porogen in the matrix/porogen hybrid dielectric film.[15] Malhouitre et al.[16] and M. Fayolle et al.[17] have demonstrated that such novel material and scheme could be achieved in a copper single damascene structure with a 25% RC reduction after porogen removal.

[a)]Address all correspondence to this author.
e-mail: jimleu@mail.nctu.edu.tw
DOI: 10.1557/JMR.2010.0136

http://journals.cambridge.org Downloaded: 25 Apr 2014 IP address: 140.113.38.11

For such a scheme, however, the decomposition temperature (T_d) of high-temperature porogen candidates needs to be higher than the maximum processing temperature (preferably at 300–400 °C) to match with the late porogen removal scheme.[18] Moreover, the mechanical strength of hybrid low-*k* material should be strong enough to pass all of the backend processing steps, especially the chemical–mechanical polish (CMP) step. Nevertheless, there is still little understanding of the interactions between high-temperature porogens and low-*k* matrix, and more importantly, there has been little research related to their effects on film structure and the properties of low-*k* materials in various stages.

Meanwhile, the thermal stability of the porogens used in the as-deposited porous low-*k* film are typically not so high that porogens can be removed readily to form porosity during dielectric deposition or subsequent thermal treatment. For example, poly(styrene-block-acrylic acid) (PS-b-PAA) with a lower decomposition temperature ($T_{d,\text{PS-b-PAA}}$: 150 °C) could be removed easily,[19] while PEO-b-PPO-b-PEO or PMMA-b-PEMAEMA may impose problems in the porosity formation because of broad decomposition range (e.g., $T_{d,\text{PEO-b-PPO-b-PEO}}$: 240–500 °C),[11] or multistage T_d from the dissimilar moieties (e.g., $T_{d,\text{PMMA-b-PEMAEMA}}$: 200 and 350 °C).[10] As for the high-temperature porogens in the late porogen removal scheme, it is desirable to attain a high and sharp decomposition temperature by incorporating stable structures such as aromatic rings or double/triple bonds as well as by using similar moieties in a block copolymer. Poly(styrene-block-4-vinylpyridine) (PS-b-P4VP) could be chosen as a good high-temperature porogen candidate because of its similar aromatic structure, which can provide a good thermal stability and desired decomposition temperature. Furthermore, different than its homopolymer statue (i.e., PS or P4VP), the amphiphilic characteristic of PS-b-P4VP could offer the advantages of microphase morphologies for controlling the pore size and pore shape by forming micelle structures.[20]

In this study, a commercial, spin-on organosilicate such as MSQ was chosen as the matrix and high-temperature porogen such as PS-b-P4VP was used as the sacrificial component. We compared the properties of several key materials among the following three types of material systems in various interconnect fabrication stages: (i) "solid-only" low-*k* materials based only on a MSQ matrix without porosity as the control, (ii) hybrid low-*k* materials (matrix + porogen), which were expected to interact with all backend processing steps, and (iii) the porous low-*k* materials after the removal of porogen presumably formed after the completion of a metal/low-*k* layer. To elucidate the impact of the porogen in the late porogen removal scheme, we first investigated the thermal stability of porogens and their impact on the processing temperatures of the MSQ/porogen hybrid and porous low-*k* materials. In addition, the porosity, dielectric, and mechanical properties of MSQ/porogen hybrid films as the starting dielectric in the late porogen removal scheme and its porous form were compared and assessed for the feasibility of their integration.

II. EXPERIMENTAL

The low-*k* material, MSQ, that was used as the matrix was obtained from Gelest Inc. (Morrisville, PA) as clear white flakes. The molecular-weight distribution of MSQ is from 6000 to 9000. PS-b-P4VP ($Mw \approx 137{,}000$; 10 wt% PS) copolymer that was used as the porogen was obtained from Sigma-Aldrich Co. (St. Louis, MO). The chemical structures of MSQ and PS-b-P4VP are illustrated by Figs. 1(a) and 1(b), respectively.

MSQ was dissolved in tetrahydrofuran (THF) to form a 5 wt% "solid-only" solution. For hybrid films, MSQ was first dissolved in n-butanol and then mixed with porogen at various loadings to form a series of 5 wt% solutions. The solutions were first filtered by a 0.20 μm polytetrafluoroethylene filter (Millipore Inc.), and then spun onto a (100) silicon wafer at 2000 rpm for 60 s at room temperature. To obtain films with better quality for subsequent tests, the solvent was removed slowly during the curing step. Therefore, the as-spun film was sequentially baked using an oven at 30, 50, 80, and 100 °C for 30 min each, then at 150 °C for 8 h. Afterward, the samples were further cured in a quartz tube furnace under a nitrogen atmosphere at a heating rate of 2 °C/min up to various final temperatures from 200 to 400 °C with an isothermal step at a 50 °C interval for 30 min each.

The study of the thermal-decomposition temperature of porogen was carried out under a nitrogen atmosphere using a TGA Q500 (TA Instruments, New Castle, DE). The temperature scan speed was 10 °C/min from 30 to 500 °C. The in situ viscosity test was measured using a rheometer (AR-1000, TA Instruments) in oscillation mode with an angular velocity of 10 rad/s at a heating rate of 2 °C/min from 30 to 200 °C.

The porosities in porous low-*k* films were measured by x-ray reflectivity (XRR). The measurements were

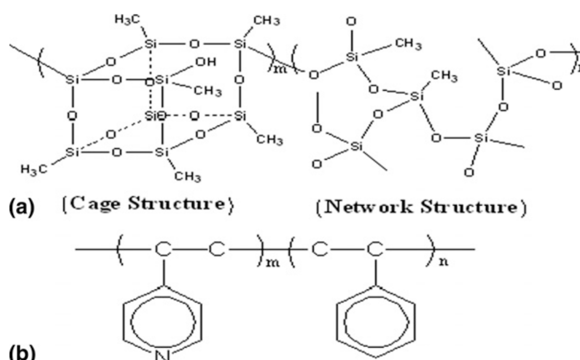

FIG. 1. The molecular structures of (a) MSQ as the low-*k* matrix, and (b) PS-b-P4VP as the high-temperature porogen.

CAMBRIDGE JOURNALS http://journals.cambridge.org Downloaded: 25 Apr 2014 IP address: 140.113.38.11

performed using a beam-line 13A1 of the National Synchrotron Radiation Research Center (NSRRC) in Taiwan. The XRR data were analyzed by LEPTOS simulation software[21] using a genetic algorithm to derive the porosities of porous MSQ films after the removal of porogens at temperatures >250 °C. The pore morphology of porous low-*k* films was examined by a dual-beam focused ion beam/scanning electron microscope (FIB/SEM) (FEI Nova 200, Hillsboro, OR) after sputtering etch ~40 nm off the surface of the low-*k* films.

Nanoindentation tests were carried out using a nanoindenter (MTS Nano Indenter XP system, Eden Prairie, MN) with a Berkovich tip in continuous mode to obtain the reduced modulus (E_r), and then the Oliver–Pharr method[22] was used to determine the elastic modulus (E) of various low-*k* films at ~1 μm thick. The chemical makeup and structural transformation in the MSQ matrix and MSQ/PS-b-P4VP porogen hybrid system as a function of temperature were studied using Fourier transform infrared spectroscopy (FTIR). The measurements were performed using a MAGNA-IR 460 (Nicolet Inc., Waltham, MA) in transmission mode with 32 scans at a 4 cm^{-1} spectral resolution.

The dielectric constant (k) of the film was measured using C–V dots based on MIS configuration [Al electrode/low-*k* film/Si (50 ohm-cm)] at room temperature in ambient by use of a Keithley 590 C–V Analyzer (Cleveland, OH) with a sweeping frequency of 100 kHz. To accurately measure the dielectric constant by C–V dot measurement, three circular aluminum dots with nominal 200, 400, and 800 μm diameters were used to minimize geometric effect. Aluminum electrodes with a thickness of 1 μm were coated onto the dielectric films by ULVAC EBX-6D thermal evaporator through a shadow mask. Measurements of film thickness were made using an n&k Analyzer 1280 (n&k Technology, Inc., San Jose, CA) at wavelengths ranging from 190 to 900 nm. For all tests except nanoindentation measurement, the typical thickness of single-coat samples is between 110 and 250 nm. For nanoindentation measurement, nominal thickness of 1 μm is used to avoid the substrate effect in the measurement.

III. RESULTS AND DISCUSSION

A. Thermal stability

The decomposition temperature of PS-b-P4VP porogen and the thermal stability of MSQ and MSQ/porogen films were first investigated to determine the maximum processing temperature of the hybrid films. The hybrid films should possess good thermal stability for subsequent dual damascene processing and porogen removal temperature after the completion of a Cu/low-*k* layer in the late porogen removal scheme. As illustrated in Fig. 2, the dynamic thermal gravimetric analyses (TGA) showed that the di-block copolymer porogen, PS-b-P4VP, had a high decomposition temperature (T_d) of ~317 °C, at which 5% weight-loss occurred and could be completely removed at $T > 380$ °C under a N_2 atmosphere. In contrast, for a MSQ/porogen hybrid system (containing 10 wt% PS-b-P4VP) as shown by Fig. 2, its T_d was increased to 325 °C, which was 8 °C higher than the decomposition temperature of pure porogen. The higher T_d in the MSQ/PS-b-P4VP system could be attributed to the intermolecular hydrogen bonding between the N atom of pyridine and the –OH group of MSQ, which in turn increased the decomposition temperature of PS-b-P4VP in the hybrid system.[23]

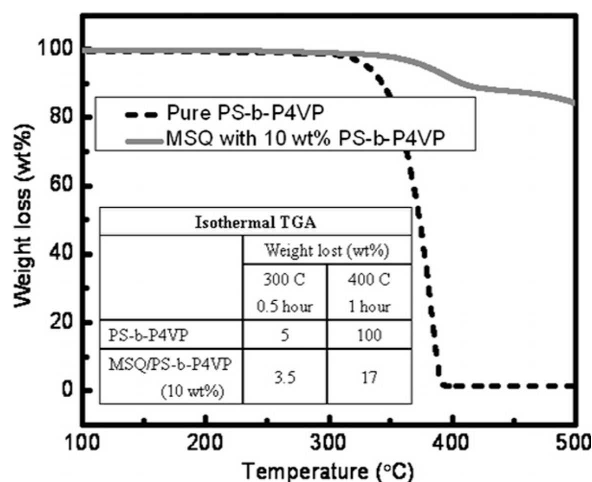

FIG. 2. The dynamic TGA curves of pure PS-b-P4VP and MSQ with 10 wt% PS-b-P4VP. Inset shows their thermal stability based on isothermal TGA data.

Since isothermal heating by hot plate or furnace is commonly used in semiconductor fabrication processing, it was confirmed that the high-temperature porogens, PS-b-P4VP, can be fully removed at $T \geq 400$ °C isothermally for 1 h using a isothermal TGA test. Furthermore, the isothermal tests of pure PS-b-P4VP and the MSQ/PS-b-P4VP hybrid system (10 wt% porogen) were also carried out at 300 °C for 30 min to examine their thermal stabilities. The table inserted in Fig. 2 shows the weight losses of pure PS-b-P4VP and MSQ/PS-b-P4VP hybrid films were 5.0 and 3.5 wt%, respectively, which are still reasonable for postdeposition processing. Based on the aforementioned thermal stability data, for the remainder of this study, hybrid MSQ/PS-b-P4VP films cured at 300 °C are designated to serve as the starting dielectric in the late porogen removal scheme, while porous MSQ low-*k* films are designated as the porous low-*k* films formed after the removal of porogen from the hybrid MSQ/PS-b-P4VP films at 400 °C.

B. Porosity and dielectric constant

Next, the effect of porogen loading on porosity was investigated using XRR to further understand the

http://journals.cambridge.org Downloaded: 25 Apr 2014 IP address: 140.113.38.11

relationship between porosity and the dielectric constant of various porous MSQ samples. Table I summarizes the correlation between porogen loading and porosity measured by XRR. The porosity of low-*k* films increased from 16.7 to 69.5 vol% as the porogen loading increased from 10 to 50 wt%.

The dielectric constant (k) of each sample was calculated from the C–V measurement results by Eq. (1), where d is the film thickness, ε_0 is the permittivity of vacuum ($\varepsilon_0 = 8.845\text{E}{-12}$), and C/A is obtained from the slope of the capacitances (C) versus different aluminum area (A) plots.[5]

$$\kappa = \frac{C}{A} \cdot \frac{d}{\varepsilon_0} \quad . \tag{1}$$

The dielectric constants of MSQ films with various porosities are summarized in Table II. The dielectric constant of the "solid-only" film or pure MSQ film was 2.82, and the k values of porous MSQ decreased from 2.72 to 2.02 when the porosity increased from 16.7 to 69.5 vol%. Nevertheless, $k < 2.5$ can be achieved by adding 40.1 vol% porosity. Moreover, ultra-low-*k* materials based on MSQ with $k = 2.0$ can be obtained when porosity of 69.5 vol% is added. A positive deviation of the dielectric constant by C–V measurement from the estimated value of the ideal mixing rule [$k_{\text{Hybrid}} = k_{\text{MSQ}} * (1 - \text{porosity}) + k_{\text{air}} * \text{porosity}$] aggravated with increasing porosity from 8.1% to 29.9% as shown by Fig. 3. This implies that as porosity increases, the pore morphology may change to connected pores, whose increased internal surface areas containing Si–OH or adsorbed water may contribute to an increase of dielectric constant because of the possibility of increased moisture uptake. Pore morphology transformation with increasing porosity is discussed further in the subsequent section.

TABLE I. Correlation between porogen loading and porosity measured by XRR.

Porogen loading (wt%)	0	10	20	30	40	50
Porosity (vol%)	0	16.7	28.8	40.1	55.2	69.5

TABLE II. The C/A value, film thickness, and dielectric constant of porous MSQ films with various porosities.

Porosity (vol%)	C/A	Drop C/A (%)	Film thickness (nm)	Dielectric constant (k)	Δk (%)
0	2.27E−4	...	110	2.82	...
16.7	2.06E−4	9.25	117	2.72	−3.55
28.8	1.74E−4	23.3	133	2.61	−7.45
40.1	1.40E−4	38.3	153	2.42	−14.2
55.2	9.02E−5	60.3	212	2.16	−23.4
69.5	7.12E−5	68.6	251	2.02	−28.4

C. Pore morphology

The pore morphology and pore sizes of various samples were investigated by SEM as shown in Figs. 4(a)–4(d). No pore appeared on the surface of the "solid-only" MSQ film shown in Fig. 4(a) because no porogen was added. When 16.7 vol% porogen was added, "wormlike" pores with a maximum size of ~70 nm were observed as shown in Fig. 4(b). As porogen loading increased from 16.7 to 40.1 vol%, or further to 69.5 vol%, the maximum pore size increased from 70 to 120 nm, and 200 nm, respectively. In addition, the shape of pores also altered from "wormlike" to "large, irregular voids" when porogen loading increased from 16.7 to 69.5 vol%. Although PS-b-P4VP porogen is an amphiphilic block

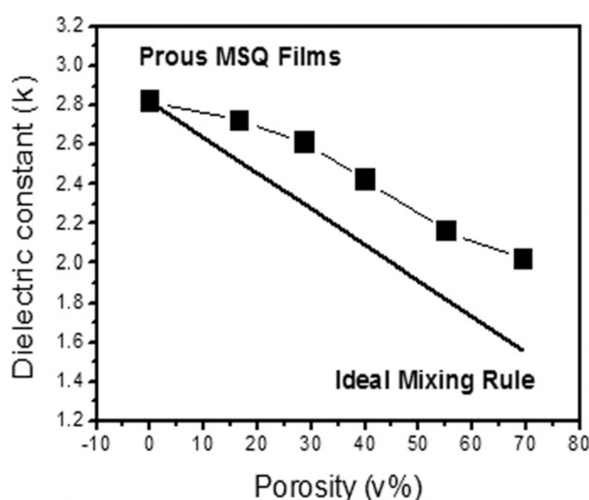

FIG. 3. The dielectric constant of porous MSQ films as a function of porosity from 0 to 69.5 vol%.

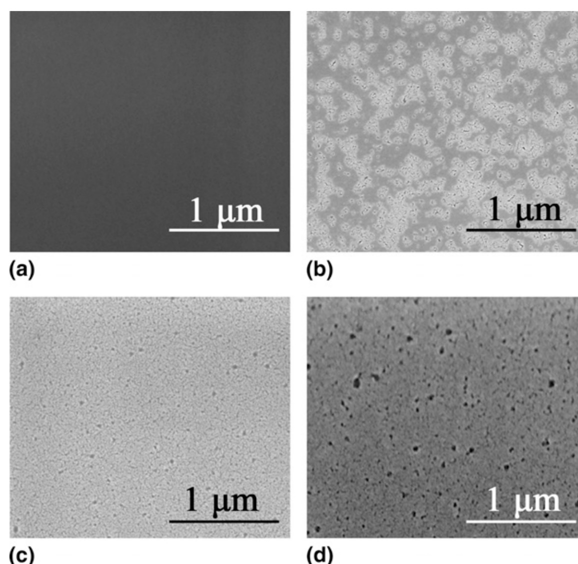

FIG. 4. The topography of porous MSQ with (a) ~0 vol%, (b) 16.7 vol%, (c) 40.1 vol%, and (d) 69.5 vol% porosity as observed by FIB/SEM after sputtering etch ~40 nm from the top of low-*k* films.

CAMBRIDGE JOURNALS
http://journals.cambridge.org Downloaded: 25 Apr 2014 IP address: 140.113.38.11

copolymer that could form a single-phase solution in n-butanol with MSQ, they would separate into two phases, i.e., MSQ moiety and PS-b-P4VP domain after solvent is removed. Moreover, in this study, the slow and multistep curing profile not only removed solvent gradually to avoid destroying the film quality, but also provided ample time for the cross-linking of MSQ and the simultaneous diffusion and aggregation of porogen.[24] Hence, at lower porosity, the formation of spherical porogen micelles was presumably disrupted by the MSQ matrix, which underwent cross-linking upon heating, and formed the wormlike pores. As the porosity increased, large quantities of porogen have more chances to aggregate together and form larger and irregular pores. However, the percolation or linkage of the pores should not affect the usefulness of this type of hybrid materials for IC applications because the high-temperature porogen, PS-b-P4VP, is removed to form porous low-*k* materials after CMP step. As long as the hybrid materials possess enough modulus to pass CMP test, it could be used in the late porogen removal scheme. Hence, the mechanical strength is further discussed in the subsequent section.

D. Mechanical strength and microstructure

The mechanical strength of low-*k* dielectric thin films is one of the critical properties in backend processing steps such as chemical–mechanical polish (CMP) and die/packaging interaction.[25] To evaluate the applicability of using hybrid MSQ/porogen film in many backend processes, elastic modulus was measured using a nanoindentation technique. The elastic moduli of the “solid-only” MSQ, hybrid (MSQ/PS-b-P4VP), and porous MSQ films as a function of porosity are shown in Fig. 5.

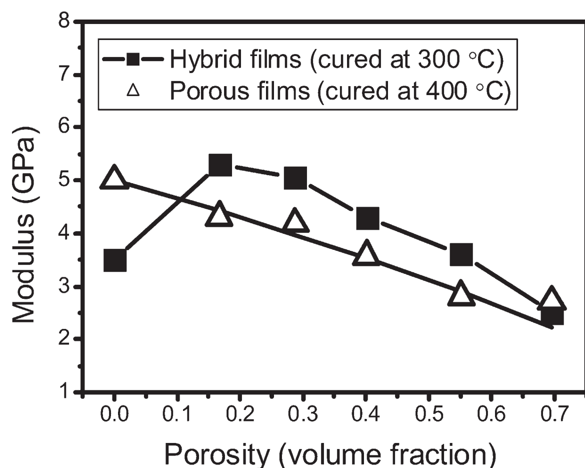

FIG. 5. The correlation between porosity and modulus for MSQ/PS-b-P4VP hybrid films cured at 300 °C and porous MSQ films cured at 400 °C.

From the results, the moduli of the porous films cured at 400 °C decreased with increasing porosity, from 5.0 GPa for “solid-only” MSQ to 2.72 GPa for 69.5 vol% porosity. The incorporation of porosity into dense low-*k* materials lowered its density, which reduced not only dielectric constant, but also mechanical properties such as elastic modulus. Interestingly, for hybrid films cured at 300 °C, the modulus for film with 16.7 vol% porogen, 5.4 GPa, was much higher than that (3.5 GPa) of the “solid-only” MSQ film cured at the same temperature. The modulus then decreased from 5.4 to 2.5 GPa with increasing PS-b-P4VP loading from 16.7 to 69.5 vol%. In general, hybrid films cured at 300 °C were stronger than those of porous MSQ for the porogen loading below 69.5 vol%. The enhanced modulus of hybrid MSQ/porogen films showed their advantage when used as ILD materials in the late porogen removal scheme, because higher modulus had a higher possibility to avoid failure during backend-end-of-line (BEOL) processes such as CMP step.

On the other hand, the measured moduli of the porous MSQ films were fitted by a semiempirical Eq. (2) derived by Phani and Niyogi,[26] where E and E_0 are the moduli at volume fraction porosity P and zero, and a and n are the material constants, respectively.

$$E = E_0(1 - aP)^n \quad . \tag{2}$$

Constant a is related to the packing geometry of the matrix and is 1 for random packing; 3.85, 2.52, and 2.1 for rhombohedral, orthorhombic, and cubic packing, respectively.[27] Because the structure of MSQ, which consists of cage and network structures, is typically amorphous or random packing, Eq. (2) can be simplified to Eq. (3):

$$E = E_0(1 - P)^n \quad . \tag{3}$$

Furthermore, the value of n is related to the pore structures. For random packing with isolated spherical pores, $a = 1$ and $n = 2$. In our study, an excellent model, $E = 5.01\ (1 - P)^{0.68}$ with a 98% goodness of fit was obtained for porous MSQ films, where the modulus of “solid-only” MSQ film was 5 GPa. The fitted n value of 0.68 ± 0.06 implies that the pore shapes are not spherical and become more interconnected as the value of n deviates greatly from 2 for spherical pores.[26] In other words, such smaller n value indicates the “wormlike” pores that are consistent with the pore morphology observed by SEM shown in Fig. 4.

To further understand how the mechanical property was affected by structural transformation in the MSQ and MSQ/porogen thin films, FTIR was used to first analyze the microstructure of pure MSQ cured at 300, 400, and 450 °C. The FTIR spectra between 1350 and 950 cm^{-1} for “solid-only” MSQ films at different curing temperatures are shown in Fig. 6. The Si–O–Si stretching

http://journals.cambridge.org Downloaded: 25 Apr 2014 IP address: 140.113.38.11

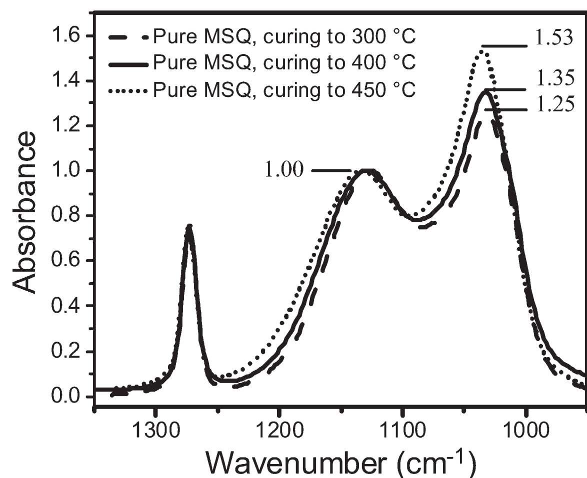

FIG. 6. The FTIR spectra of "solid-only" MSQ films cured at various temperatures in the range of 950 to 1350 cm^{-1}.

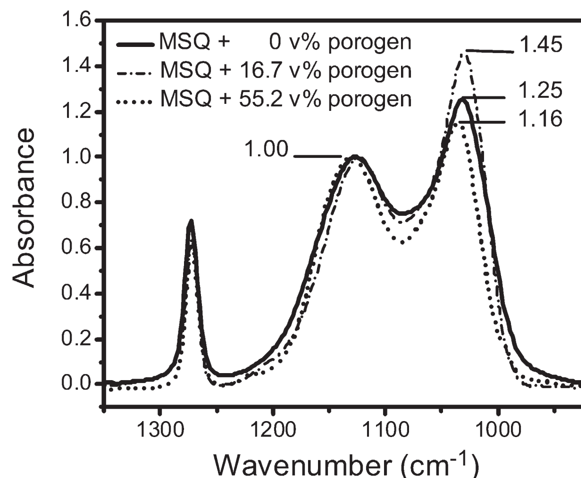

FIG. 7. The FTIR spectra of the hybrid MSQ/PS-b-P4VP low-*k* films cured at 300 °C in the range of 950 to 1350 cm^{-1}.

peaks at 1130 and 1030 cm^{-1} were assigned to the cage and network structures, respectively. The network/cage ratio was found to increase from 1.25 to 1.53 with increasing curing temperatures from 300 to 450 °C. It has been reported that the structure of three dimensional cross-linking Si–O–Si (network structure) is more stable and stronger than polyhedral Si–O–Si (cage structure).[28] Hence, the network/cage structural ratio of the Si–O–Si peaks was a good indicator of the degree of cross-linking and thus the mechanical strength. Therefore, the main difference among the "solid-only" MSQ cured at 300, 350, or 400 °C is in their network/cage structural ratios, which play a critical role in their mechanical strength and yield 3.5 and 5.0 GPa for curing at 300 and 400 °C, respectively.

The FTIR analysis was also carried out for the hybrid MSQ/porogen films with various porogen loadings to study whether there is any interaction between MSQ and PS-b-P4VP. Figure 7 shows the network/cage structural ratios of the Si–O–Si peaks between 1350 and 950 cm^{-1} for hybrid MSQ/porogen films with different loadings cured at 300 °C. The network/cage ratio was found to increase from 1.25 for pure MSQ to 1.45 for 16.7 vol% porogen, and then dropped to 1.16 when 55.2 vol% porogen was added. It appears that the tendency of the network/cage ratio as a function of porosity matches that of the modulus of hybrid films.

Therefore, to explore any correlation between network/cage structural ratios and moduli of hybrid MSQ/porogen films, network/cage structural ratios and moduli as a function of porosities are plotted in Fig. 8. The network/cage ratio increased from 1.25 for "solid-only" MSQ at 300 °C to 1.45 for 16.7 vol% porogen loading, which correlated well with the significant increase of mechanical strength from 3.5 to 5.4 GPa, because of the increase in the degree of MSQ cross-linking. For loading above 16.7 vol%, the network/cage structural ratio decreased from 1.45 to

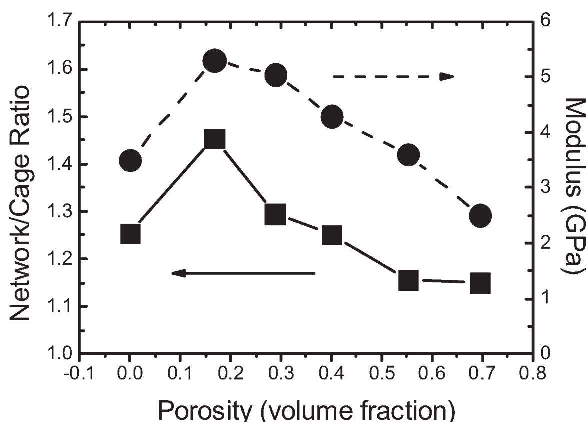

FIG. 8. The network/cage ratio and modulus versus porosity at various porogen loading for hybrid MSQ/PS-b-P4VP low-*k* films cured at 300 °C.

1.15 with the increase of porogen loading from 16.7 to 69.5 vol%, which confirmed the corresponding trend of the modulus. For porogen loadings below a critical quantity (i.e., ~69.5 vol% for PS-b-P4VP), porogen may act as a plasticizer, which could provide better mobility for MSQ molecular chains to come close and cross-link to form more network structure.

To elucidate the plasticization effect, viscosity of pure MSQ and MSQ/PS-b-P4VP (16.7 vol%) system as a function of temperature during cure step was measured. Figure 9(a) shows the viscosity of pure MSQ from 30 to 200 °C increased from 1.1×10^3 to 2.3×10^5 because of the removal of solvent and the cross-linking of MSQ when temperature was raised from 50 to 150 °C. After that, the viscosity of pure MSQ reached a stable state because the structure of MSQ was frozen by complete cross-linking. In contrast, for hybrid system, four regions of viscosity could be observed in Fig. 9(b). In region (I), the solvent decreased with increasing temperature from

http://journals.cambridge.org Downloaded: 25 Apr 2014 IP address: 140.113.38.11

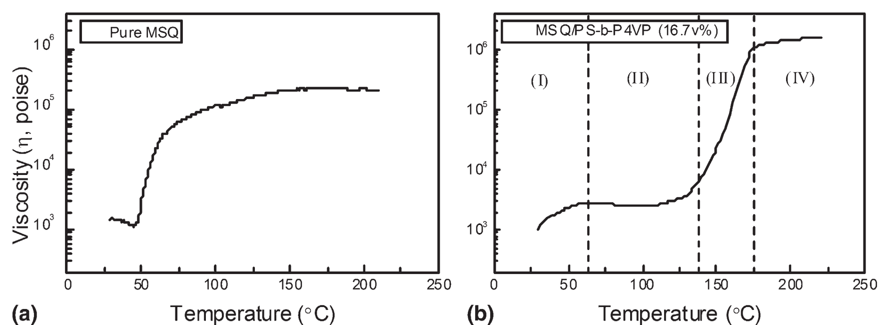

FIG. 9. The viscosity of (a) pure MSQ and (b) MSQ/PS-b-P4VP (16.7 vol%) system as a function of the temperature.

30 to 65 °C, leading to an increase of viscosity from 1.0×10^3 to 2.8×10^3 P. Then, the viscosity maintains at relatively low value (2.8×10^3 to 3.5×10^3 P) for temperature between 65 and 135 °C in the region (II). In this region, lower viscosity implies that little cross-linking of MSQ occurs. The molecular chain of MSQ can still move via solvent and porogen over such temperature domain. On the other hand, T_g of the pure PS-b-P4VP is 100 °C for PS and 150 °C for P4VP.[29] Therefore, the PS-b-P4VP copolymer can provide better mobility for MSQ molecular chains under a curing temperature exceeding 117 °C, the boiling point of n-butanol. After that, in region (III), the viscosity increased three orders from 3.5×10^3 to 1.0×10^6 poise when temperature was increased from 135 to 175 °C. This implies the MSQ starts drastic cross-linking in this temperature domain. Such temperature domain of drastic cross-link is similar to that reported in the literatures.[12,30] Finally, the molecular chain of cross-linked MSQ has been frozen and hard to move. Therefore, the viscosity increased slightly with increasing temperature in the region (IV). Based on the rheometry results, we believe that the porogen could act like a plasticizer after the solvent is removed in region (II).

However, as porogen loading increased, the presence of porogen also became a steric barrier for MSQ molecular chains, thus reducing the collision probability of MSQ molecular chains for further cross-linking. Therefore, the reduced degree of cross-linking in MSQ with porogen loading greater than 69.5 vol% could account for its lower mechanical strength, even compared with those of porous MSQ cured at 400 °C. To sum up, depending on the volume fraction of porogen, porogen acted as a plasticizer, which provided a better mobility for MSQ molecular chains to come close and thus facilitated cross-linking to form more networking structure chains with higher mechanical strength at low porogen loadings. Moreover, porogen also acted as a roadblock to the collision of MSQ molecular chains for cross-linking, which reduced mechanical strength with high porogen loadings.

Finally, we assessed how these novel hybrid low-*k* films would fare during chemical-mechanical polish steps based on the study in SEMATEC by Wetzel et al., in which low-*k* material could pass the CMP test if its modulus is larger than 4 GPa.[31] For porous MSQ films cured directly at 400 °C, the modulus of porous film became lower than 4 GPa when porogen loading was higher than 29 vol%. In contrast, hybrid low-*k* films prepared by the late porogen removal scheme, i.e., cured at 300 °C, possessed modulus higher than 4 GPa for an even larger porosity of ∼45 vol%. That means we can use the same matrix and porogen to design and produce ILDs with high porosity when the modulus is sufficient to survive backend processes such as CMP step using the late porogen removal scheme. Meanwhile, there is a possibility of avoiding the barrier reliability issue altogether because of the large pore sizes formed immediately during the burn-out step after ILD film deposition. However, this possibility is yet to be validated experimentally.

IV. CONCLUSIONS

A late porogen removal scheme was used to make low-*k* materials ($k = 2.72$ to 2.02) using MSQ, and a high-temperature porogen, PS-b-P4VP, was used to circumvent the reliability issues related to as-deposited porous dielectric. Based on the dynamic and isothermal TGA data, it was recommended that the hybrid MSQ/PS-b-P4VP material system to be cured at 300 °C for subsequent backend processes with reduced thermal budget ≤300 °C, and the porogen be removed at 400 °C for 1 h after the completion of a metal/dielectric layer. Moreover, dielectric constants of ultralow-*k* MSQ/PS-b-P4VP films using slow, multistep curing profile deviated from the ideal mixing rule with increasing porogen loading. This is presumably because of the changed pore morphology or interconnected pores. Finally, for porogen loading below a critical level (∼69 vol%), the modulus of hybrid films was higher than their porous forms, and even better than the "solid-only" MSQ. This can be attributed to their enhanced degree of cross-linking in the MSQ matrix resulting from the plasticization caused by the PS-b-P4VP porogen. This implies that hybrid low-*k* materials systems can pass the CMP test

CAMBRIDGE JOURNALS
http://journals.cambridge.org Downloaded: 25 Apr 2014 IP address: 140.113.38.11

(elastic modulus >4 GPa) while avoiding the barrier reliability issue. In addition, more aggressive *k* reduction without failing CMP tests can be achieved using a hybrid low-*k* materials system.

ACKNOWLEDGMENTS

The authors wish to thank the financial support in part by National Science Council of ROC under Contract Nos. NSC97-2221-E009-160 and NSC98-2221-E009-177 and a research grant from Taiwan Semiconductor Manufacturing Company, Ltd. (TSMC) of ROC. Beamline 13A1 support for x-ray reflectivity from National Synchrotron Radiation Research Center (NSRRC) in Taiwan is also acknowledged.

REFERENCES

1. M.T. Bohr: Interconnect scaling—The real limiter to high performance ULSI. *IEEE IEDM* 241 (1995).
2. C.K. Hu and J.M.E. Harper: Copper interconnections and reliability. *Mater. Chem. Phys.* **52,** 5 (1998).
3. P. Gonon, A. Sylvestre, H. Meynen, and L. Van Cotthem: Permittivity and conductivity of low-dielectric constant SiOC:H films deposited by plasma-enhanced chemical vapor deposition. *J. Electrochem. Soc.* **150,** F47 (2003).
4. S.J. Martin, J.P. Godschalx, M.E. Mills, E.O. Shaffer II, and P.H. Townsend: Development of a low-dielectric constant polymer for the fabrication of integrated circuit interconnect. *Adv. Mater.* **12,** 1770 (2000).
5. P.S. Ho, J. Leu, and W.W. Lee: *Low Dielectric Constant Materials for IC Applications* (Springer, New York, 2002).
6. C.C. Chiang, M.C. Chen, C.C. Ko, S.M. Jang, C.H. Yu, and M.S. Liang: Physical and barrier properties of plasma-enhanced chemical vapor deposited α-SiCN:H films with different hydrogen contents. *Jpn. J. Appl. Phys.* **42,** 5246 (2003).
7. Executive Summary Semiconductor Industry Association: *International Technology Roadmap for Semiconductors* (2007).
8. A.M. Padovani, L. Rhodes, S.A.B. Allen, and P.A. Kohl: Chemically bonded porogens in methylsilsesquioxane: I. Structure and bonding. *J. Electrochem. Soc.* **149,** F161 (2002).
9. S. Baskaran, J. Liu, K. Dormansky, N. Kohler, X. Li, C. Coyle, G.E. Fryxell, S. Thevuthasan, and R.E. Williford: Low-dielectric constant mesoporous silica films through molecularly templated synthesis. *Adv. Mater.* **12,** 291 (2000).
10. H.C. Kim, J.B. Wilds, C.R. Kreller, W. Volksen, P.J. Brock, V.Y. Lee, T. Magbitang, J.L. Hedrick, C.J. Hawker, and R.D. Miller: Fabrication of multilayered nanoporous poly(methyl silsesquioxane). *Adv. Mater.* **14,** 1637 (2002).
11. S. Yang, P.A. Mirau, C.S. Pai, O. Nalamasu, E. Reichmanis, J.C. Pai, Y.S. Obeng, J. Seputro, E.K. Lin, H.J. Lee, J. Sun, and D.W. Gidley: Nanoporous ultralow-dielectric constant organosilicates templated by triblock copolymers. *Chem. Mater.* **14,** 369 (2002).
12. Q.R. Huang, H.C. Kim, E. Huang, D. Mecerreyes, I.L. Hedrick, W. Volksen, C.W. Frank, and R.D. Miller: Miscibility in organic/inorganic hybrid nanocomposites suitable for microelectronic applications: Comparison of modulated differential scanning calorimetry and fluorescence spectroscopy. *Macromolecules* **36,** 7661 (2003).
13. P. Lazzeri, L. Vanzetti, M. Anderle, M. Bersani, J.J. Park, Z. Lin, R.M. Briber, G.W. Rubloff, H.C. Kim, and R.D. Miller: Thin-film transformations and volatile products in the formation of nanoporous low-k polymethylsilsesquioxane-based dielectric. *J. Vac. Sci. Technol., B* **23,** 908 (2005).
14. K. Mosig, T. Jacobs, K. Brennan, M. Rasco, J. Wolfe, and R. Augur: I ntegration challenges of porous ultra low-*k* spin-on dielectrics. *Microelectron. Eng.* **64,** 11 (2002).
15. J. Calvert, M. Gallagher, T. Adams, A. Pandit, G. Prokopowicz, C. Sullivan, and H. Zhen: *Zirkon Porous Ultra Low-K Dielectrics* (Shipley Co., Marlborough, MA, 2003).
16. S. Malhouitre, C. Jehoul, J. Van Aelst, H. Struyf, S. Brongersma, L. Carbonell, I. Vos, G. Beyer, M. Van Hove, D. Gronbeck, M. Gallagher, J. Calvert, and K. Maex: Single damascene integration of porous Zirkon version 1 low-k dielectric films. *Microelectron. Eng.* **70,** 302 (2003).
17. M. Fayolle, V. Jousseaume, M. Assous, E. Tabouret, C. le Cornec, P.H. Haumesser, P. Leduc, H. Feldis, O. Louveau, G. Passemard, and F. Fusalba: Cu/ULK integration using a post integration porogen removal approach. *IEEE IITC* 208 (2004).
18. S.P. Murarka, M. Eizenberg, and A.K. Sinha: *Interlayer Dielectrics for Semiconductor Technologies* (Elsevier/Academic Press, San Diego, CA, 2003).
19. Y. Chang, C.Y. Chen, and W.C. Chen: Poly(methyl silsesquioxane)/amphiphilic block copolymer hybrids and their porous derivatives: Poly(styrene-block-acrylic acid) and poly(styrene-block-3-trimethoxysilylpropyl methacrylate). *J. Polym. Sci., Part B: Polym. Phys.* **42,** 4466 (2004).
20. I.W. Hamley: *The Physics of Block Copolymers* (Oxford University Press, Oxford, UK, 1998).
21. A. van der Lee, F. Salah, and B. Harzallah: A comparison of modern data analysis methods for x-ray and neutron specular reflectivity data. *J. Appl. Crystallogr.* **40,** 820 (2007).
22. W.C. Oliver and G.M. Pharr: An improved technique for determining hardness and elastic modulus using load and displacement sensing indentation experiments. *J. Mater. Res.* **7,** 1564 (1992).
23. C.C. Yang, P.T. Wu, W.C. Chen, and H.L. Chen: Low-dielectric constant nanoporous poly(methyl silsesquioxane) using poly (styrene-block-2-vinylpyridine) as a template. *Polymer (Guildf.)* **45,** 5691 (2005).
24. G.J.A.A. Soler-Illia and P. Innocenzi: Mesoporous hybrid thin films: The physics and chemistry beneath. *Chem. Eur. J.* **12,** 4478 (2006).
25. J. Tan, Z.W. Zhong, and H.M. Ho: Wire-bonding process development for low-k materials. *Micro. Eng.* **81,** 75 (2005).
26. K.K. Phani and S.K. Niyogi: Young's modulus of porous brittle solids. *J. Mater. Sci.* **22,** 257 (1987).
27. K.K. Phani, S.K. Niyogi, and A.K. De: Porosity dependence of fracture mechanical properties of reaction sintered Si_3N_4. *J. Mater. Sci. Lett.* **7,** 1253 (1988).
28. S. Kim, Y. Toivola, R.F. Cook, K. Char, S.H. Chu, J.K. Lee, D.Y. Yoon, and H.W. Rhee: Organosilicate spin-on glasses: I. Effect of chemical modification on mechanical properties. *J. Electrochem. Soc.* **151,** F37 (2004).
29. C.F. Huang, S.W. Kuo, J.K. Chen, and F.C. Chang: Synthesis and characterization of polystyrene-b-poly(4-vinyl pyridine) block copolymers by atom transfer radical polymerization. *J. Polym. Res.* **12,** 449 (2005).
30. J.K. Lee, K. Char, H.W. Rhee, H.W. Ro, D.Y. Yoo, and D.Y. Toon: Synthetic control of molecular weight and microstructure of processible poly(methylsilsesquioxane)s for low-dielectric thin film applications. *Polymer (Guildf.)* **42,** 9085 (2001).
31. J.T. Wetzel, S.H. Lin, E. Mickler, J. Lee, B. Ahlbum, C. Jin, R.J. Fox III, M.H. Tsai, W. Mlynko, K.A. Monnig, and P.M. Winebarger: Evaluation of material-property requirements and performance of ultra-low-dielectric constant insulators for inlaid copper metallization. *IEEE IEDM* 73 (2001).

CAMBRIDGE JOURNALS
http://journals.cambridge.org Downloaded: 25 Apr 2014 IP address: 140.113.38.11